

Fluorescence strategies for high-throughput quantification of protein interactions

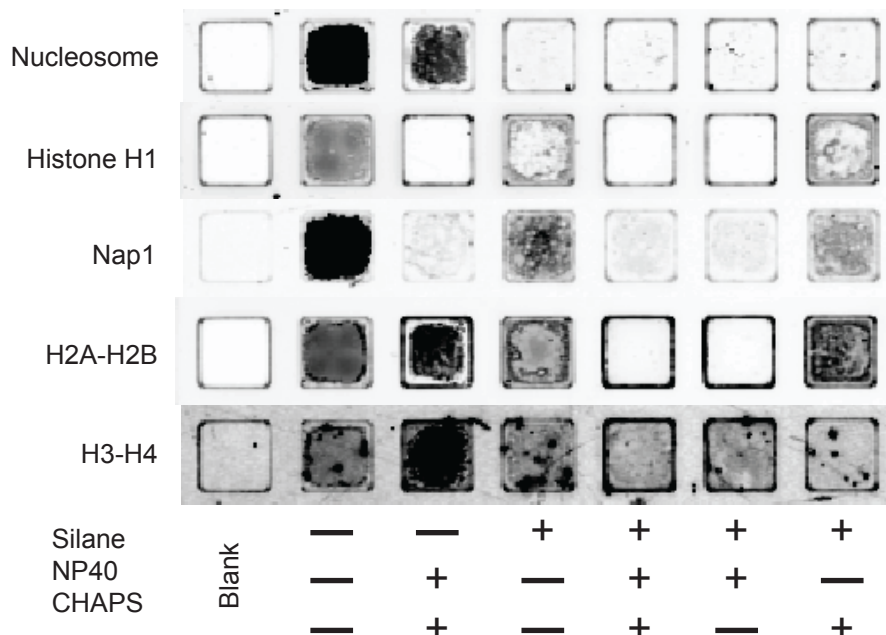
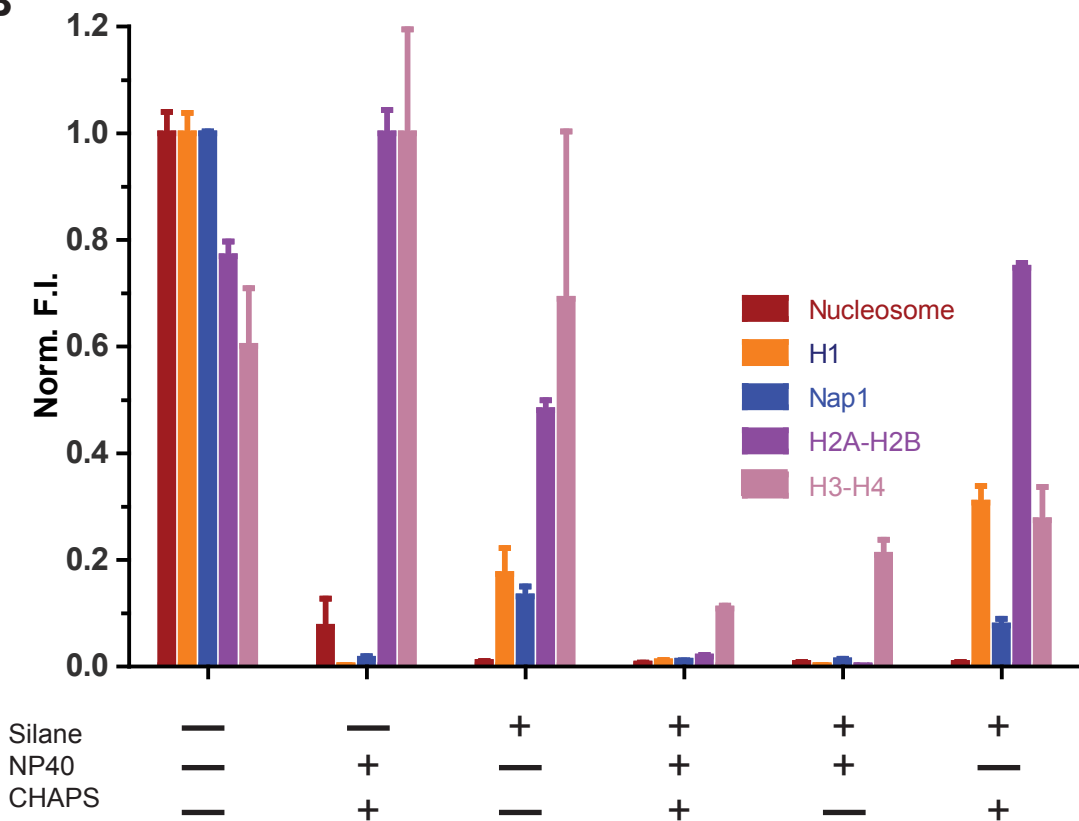
Supplementary Information

Aaron R Hieb, Sheena D'Arcy, Michael A Kramer, Alison E White, Karolin Luger

Supplementary Table 1: Summary of thermodynamic binding constants shown in Figures 2-4.

Histone H1 (Fig. 2)	K_D (nM)	Hill
207 bp DNA	4.3 ± 0.6	1.97 ± 0.06
207 bp Nucleosome	1.2 ± 0.3	0.9 ± 0.3
PARP1 (Fig. 3)	K_D (nM)	Hill
30bp Blunt (175 mM KCl)	18 ± 3	N/A
30bp Blunt (200 mM KCl)	60 ± 10	N/A
30bp Blunt (225 mM KCl)	131.4 ± 0.14	N/A
30bp Blunt (250 mM KCl)	210 ± 10	N/A
Nap1 (affinity) (Fig. 4B)	K_D (nM)	Hill
H2A/H2B	9.9 ± 2	0.8 ± 0.1
Nap1 competition (Fig. 4C)	IC₅₀ (nM)	Hill
Nap1(WT)	250 ± 50	.90 ± .05
Nap1(1-365)	570 ± 60	0.64 ± .04
Nap1(74-417)	1060 ± 30	0.875 ± .007
Nap1(74-365)	6200 ± 800	1.2 ± 0.2

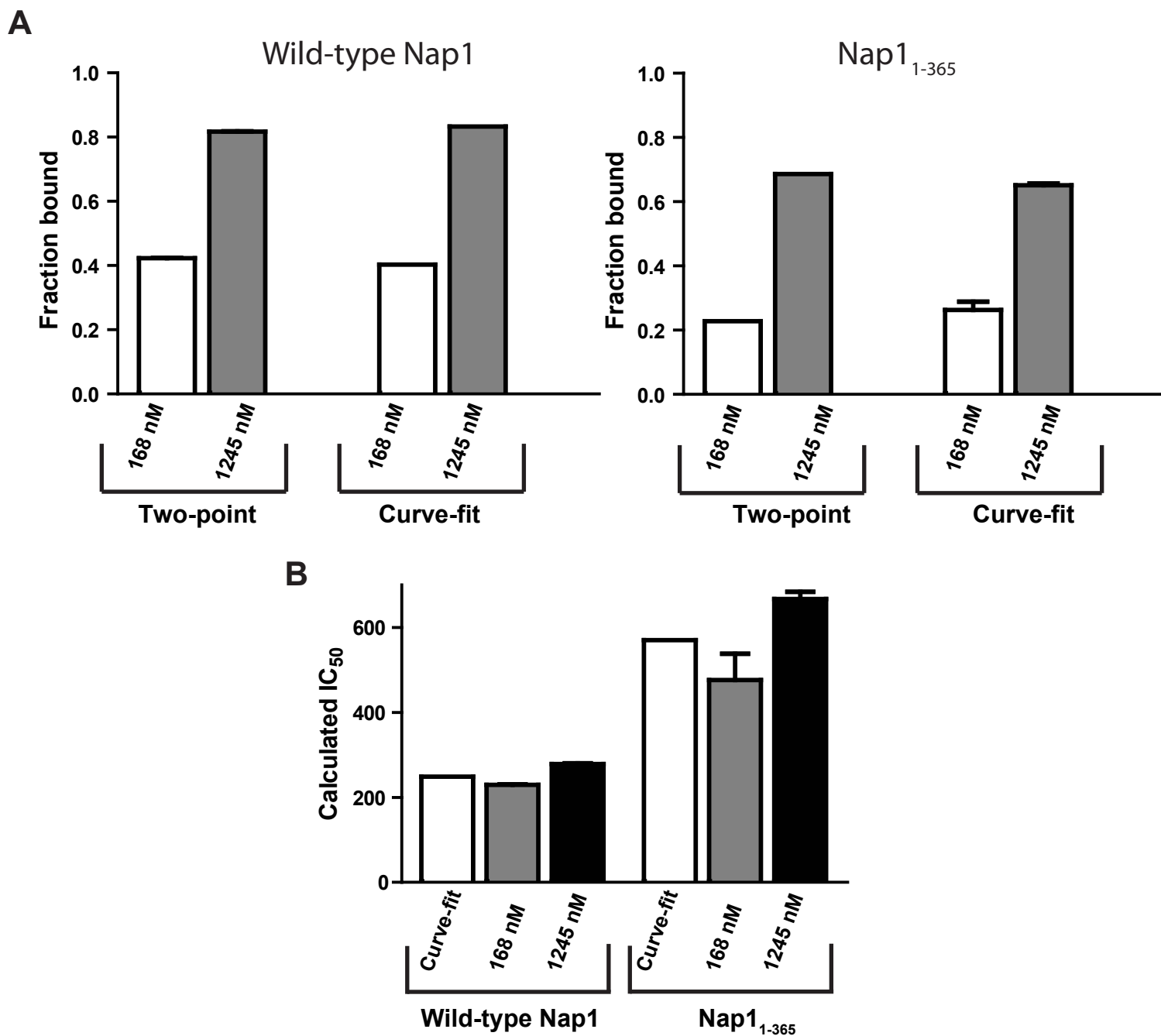
* Errors represent the range or standard deviation between two or more replicate experiments, with each experiment containing 2-4 replicate titrations.

A**B**

Supplementary Figure 1. The combination of hydrophobic silanization with detergents prevents protein adsorption to the microplate surface. **A)** Microplate wells incubated with 20 nM of specified proteins with or without NP40 and/or CHAPS detergents, and/or hydrophobic silane passivation. After incubation with protein, wells were washed 6-times with the incubation buffer to remove nonadsorbed protein. **B)** Quantification of the data in (A). A combination of silanization, 0.01% NP40, and 0.01% CHAPS has the largest and broadest effect on surface sticking with the proteins tested.

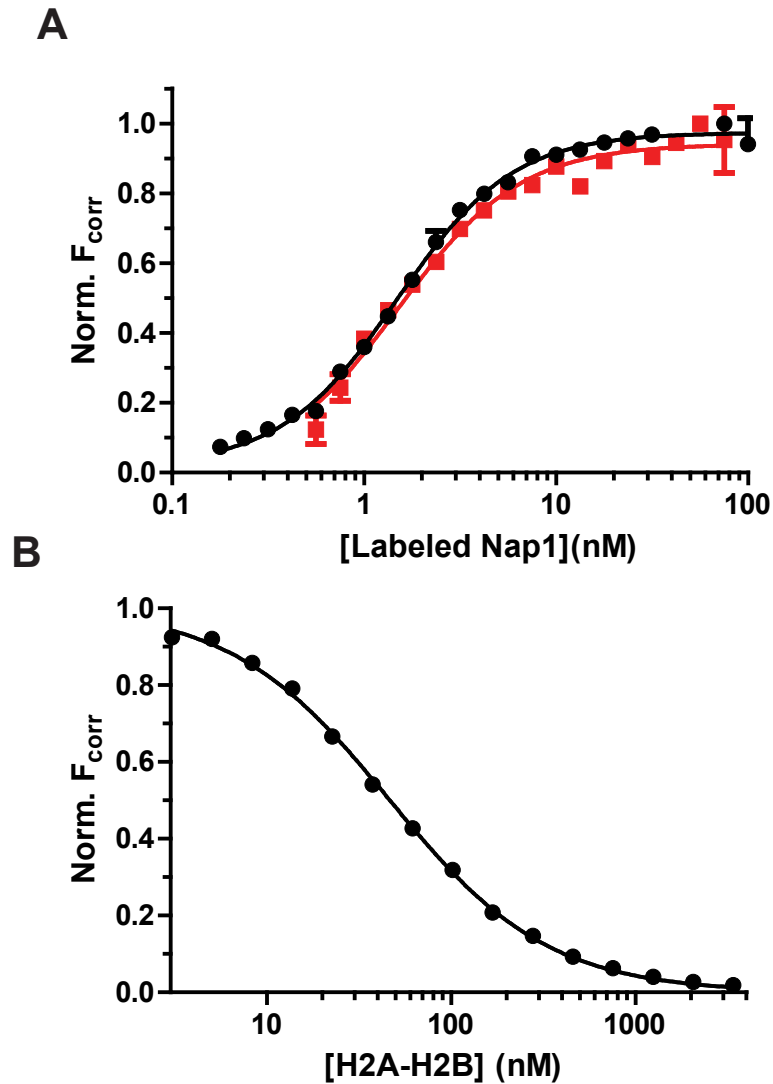
A**B**

Supplementary Figure 2. Schematics depicting the consequences of protein and DNA-ligand titration. A) Protein titration onto a labeled DNA substrate and the subsequent buildup of nonspecific interactions. B) DNA titration onto labeled protein substrate, allowing specific binding to the DNA and avoiding the buildup of nonspecific interactions. Green star indicates which molecule is the labeled probe.

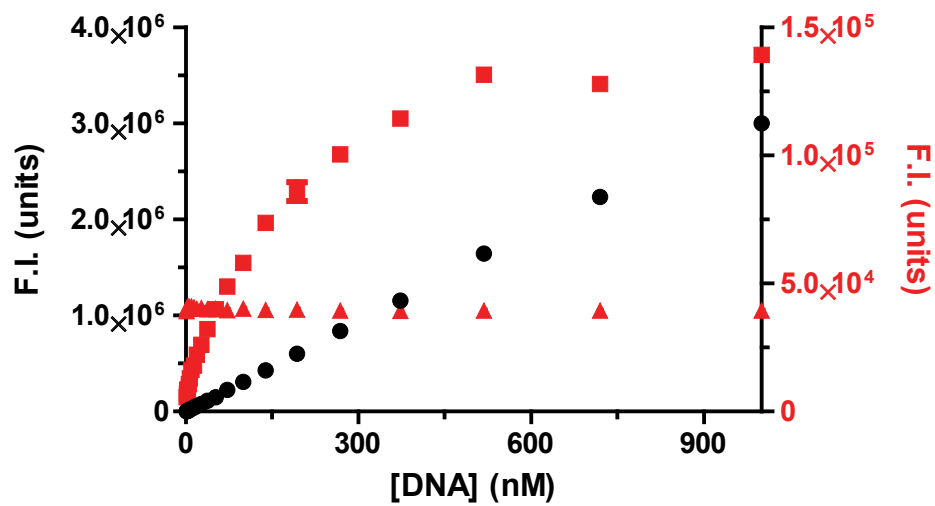


Supplementary Figure 3. A two-point assay can be used to determine relative binding affinities.

A) Select data points at 168 nM and 1245 nM from the F_{corr} curves in Fig. 4C for Nap1 wild-type and mutant Nap1₁₋₃₆₅ constructs, plotted as fraction bound; points can be compared to the predicted values from the curve-fit. **B)** The data from (A) as calculated into predicted IC₅₀ values, or derived from curve-fitting a full data-set. Regardless of which titration point was tested, the IC₅₀ values are very similar to the values determined from fitting a full-titration curve.



Supplementary Figure 4. A) A titration of $H2A-H2B_{Donor}$ with 1 nM $Nap1_{Acceptor}$ (■) gives rise to the same binding curve as an experiment titrating $Nap1_{Acceptor}$ with 1 nM $H2A-H2B_{Donor}$ (●). **B)** Unlabeled $H2A-H2B$ can compete for binding between $H2A-H2B_{Donor}$ (50 nM) and $Nap1_{Acceptor}$ (10 nM).



Supplementary Figure 5. The contribution of spectral overlap in a FRET calculation. A plot showing the intensities of Fcorr (■), Donor bleed-through (▲), and Acceptor direct excitation (●) values from the data in (A and B). Direct excitation is plotted on the left y-axis, whereas bleed-through and Fcorr are plotted on the right y-axis

Supplementary Methods

1. Suppression of nonspecific interactions with the microplate surface – passivation of microplates

Despite these high-throughput and in-solution advantages, microplates are not without caveats. For example, the glass bottom is prone to protein adsorption or ‘sticking’, potentially resulting in changes in fluorescence unrelated to the binding event being measured. The phenomenon is often aggravated by the presence of fluorophores, and is particularly worrisome at the low concentrations that are typically required in fluorescence assays. Moreover, histones and other highly charged proteins are particularly notorious for their propensity to adsorb to glass and plastic surfaces. Therefore, ‘low binding’ tips and tubes should always be used to limit any adsorption prior to addition into the microplate.

We have found that coating the surface of the microplate with a hydrophobic layer and combining small amounts of nonionic and ionic detergents greatly alleviates sticking. Specifically, adsorption is prevented by passivating the glass-bottom surface of each well with hydrophobic silane (1,7-Dichlorooctamethyl-tetrasiloxane; Sigma). This, together with adding small amounts of nonionic (0.01% Nonidet-P40 substitute) and ionic (0.01% CHAPS detergent) detergents to the reaction buffer, as described in the **Methods**, greatly reduces adsorption. **Supplementary Fig. 1** compares surface adsorption with a variety of labeled protein samples with and without surface treatment and detergents. Proteins were incubated for 20 minutes at 20 nM in each well in 150 mM KCl binding buffer, with and without detergents or passivation. Wells were then washed five times with the same 150 mM KCl binding buffer. The surface was visualized on a Typhoon imager, with settings specific for each fluorophore attached to the protein of interest. This experiment clearly shows that surface silanization and both types of detergents in the binding buffer are essential or eliminating nearly all the protein-surface interactions. For example, H2A-H2B adsorbs strongly to untreated microplates in the absence of detergents. Further addition of either silane passivation or detergents is not enough to prevent sticking; only the combination of silane and detergents prevents sticking. Notably, NP40 appears to have the largest effect on the suppression of sticking, but the presence of CHAPS aids in further suppression for some proteins (i.e. histone (H3-H4)). Therefore, for consistency, we typically add both NP40 and CHAPS detergents to all reactions. While we cannot visualize the side of the chamber, we believe that it is also well silanized based upon physical observation and the fact that the chlorinated silane is highly reactive to a variety of functional groups, including alkyl benzenes (44). Notably, for silanization we clean with Hellmanex and KOH, where the Hellmanex removes all oily organic residues on the surface and the KOH both etches (smoothes) and activates the glass surface creating a uniform hydroxyl layer for the silane to react with.

2. Suppression of nonspecific protein-nucleic acid interactions

DNA-binding proteins regulate many cellular processes, relying on finely tuned affinities of various proteins for different DNA-binding motifs. Discerning the subtle differences between different DNA-binding modules for specific sites on the DNA has been difficult, especially for proteins that exhibit a high propensity for nonspecific DNA association (45). Historically, protein-DNA interactions have been measured by titrating unlabeled protein into a constant concentration of DNA probe, as shown in schematically in **Supplementary Figure 2A**. However, since most DNA binding proteins bind nucleic acids nonspecifically with significant affinities, a buildup of multiple proteins on a single DNA molecule can occur, convoluting the interpretation of the data (6). To overcome this limitation, affinity measurements can be performed with labeled protein as the probe (generally at concentrations more than ten-fold below the K_D), while titrating the DNA as the substrate, as shown in **Supplementary Figure 2B**; for examples see Andrews et al., 2010 (46) and Fan et al., 2007 (47). Thus, nonspecific interactions are disfavored, allowing the protein to bind a single DNA substrate and associate only with the highest-affinity binding site. Another advantage of this approach is that the specific activity of the protein does not need to be taken into account, because the protein is the labeled substrate and a decrease in activity will only reduce signal change, not the effective concentration of what is being titrated. A similar approach can be applied to protein-protein complexes; the protein with a tendency for non-specific, lower-affinity interactions should be used as the probe.

3. Using F_{corr} vs. Efficiency Transfer

In the experiments described in the main text, we have chosen to plot F_{corr} rather than efficiency transfer (E) to minimize the number of required control reactions and to simplify data processing. F_{corr} is readout of only the final bound state of all components as explained in **Methods**. However, when calculating E , various factors have to be controlled for, including quenching and anisotropy changes, as well as detection efficiency (10). A correction factor (γ) is used as a normalization factor to keep the denominator from changing in the efficiency transfer equation; γ is composed of the instrument detection efficiency, acceptor labeling efficiency, and the ratio of quantum yields between the dyes. Correcting with γ ensures that every photon transferred from the donor fluorophore is collected with equal efficiency in the FRET channel:

$$E = \left(\frac{F_{corr}}{F_{corr} + \gamma \cdot D} \right) \quad (1)$$

If the correction factor γ is not applied, a changing denominator results in a skewed reflection of the fractional binding; thus, changes in labeling efficiency or distance between fluorophores will result in a change in the observed K_D . As an example of this, **Fig. 1C** shows multiple theoretical binding curves where γ and efficiency transfer values are changed. From this we

observe significant changes in binding affinity, showing how changes in the system (e.g. labeling percentage, channel detection efficiency, or distance between fluorophores) can create variability in replicate measurements. For example increasing γ to 2 will show a decreased binding affinity. Likewise, if γ does not equal 1, a change from 0.1 to 0.5 efficiency transfer will also decrease the observed K_D .

4. Comparison of IC_{50} raw and corrected data

When using HI-FI competition assays for IC_{50} determination, either the raw FRET data, background subtracted FRET data, or overlap corrected (F_{corr}) values can be plotted. This is shown in **Fig. 4E,F**, where uncorrected values give similar, but not identical, results. Therefore, one must use caution when working with the raw or background subtracted data, because the observed data can be skewed from those of the actual F_{corr} values. Using the overlap corrected values is also advantageous because the F_{corr} signal should drop to zero upon complete competition. If this is not the case, quenching or an alternative effect could be causing a decrease but not complete loss of F_{corr} .

5. Two-point assay

The K_D as well as the degree of cooperativity can be extracted from binding isotherms, however this level of information is not required for all applications, and two-point assays can be performed to increase throughput and decrease sample consumption. This entails using the FRET competition assay as described, but instead of performing a full titration, the unlabeled competitor is added at the concentration of the expected IC_{50} for unlabeled wild-type. Based on the fraction remaining bound and a theoretical IC_{50} curve, one can obtain a rough estimate for the K_D relative to the wild-type. We show an example of this in **Supplementary Fig. 3**, where we picked single points (Y) from the titration curves for wild-type Nap1 or Nap1₇₄₋₄₁₇ shown in **Fig. 4C** and determined the fraction bound (FB), based upon the initial F_{corr} signal (Y_{max}), provided that the plateau at full competition equals zero:

$$FB = \left(\frac{Y_{max} - Y}{Y_{max}} \right) \quad (2)$$

When using a two point assay, the IC_{50} can be calculated as follows ($[X] = [\text{labeled Nap1}]$):

$$IC_{50} = \left(\frac{[X]}{1 - FB} \right) - [X] \quad (3)$$

When comparing points taken at 56 nM and 237 nM, we find nearly identical results (**Supplementary Fig. 3B**) to those obtained from full titration curves. Using this type of methodology, one can rapidly and quantitatively determine the effect of a specific mutation. We speculate that the competition assay will also work with relatively crude protein purifications.

6. Donor titration

We have demonstrated the utility of the HI-FI-FRET assay, where fluorescence acceptor is titrated. However in many cases, testing of the donor labeled protein is also of interest. For example, donor titrations would allow affinity measurements of the donor labeled protein without having to switch the label. To determine whether this is possible with the HI-FI system, we performed a binding affinity measurement for the (H2A-H2B)-Nap1 interaction using a titration with H2A-H2B_{Donor}, while keeping Nap1_{Acceptor} below the K_D (**Supplementary Fig. 4A**). From this experiment we were able to determine binding affinities that matched those from a Nap1_{Acceptor} titration. This experiment highlights how a donor titration is a viable method to obtain binding affinities.

Likewise, when performing FRET competition experiments, the donor labeled protein can also be competed for binding, making further characterization of the complex easier. To show the applicability of this approach, we performed an experiment where Nap1_{Acceptor} (10 nM) and H2A-H2B_{Donor} (50 nM) are combined and the interaction competed with unlabeled H2A-H2B. **Supplementary Fig. 4B** shows a plot of the overlap corrected FRET values with which we determine an IC_{50} of 46 nM, which is nearly identical to the predicted value of 59 nM. This shows that either the acceptor or donor labeled proteins can be competed for interaction.

Supplementary References

10. Lee, N.K., Kapanidis, A.N., Wang, Y., Michalet, X., Mukhopadhyay, J., Ebright, R.H. and Weiss, S. (2005) Accurate FRET measurements within single diffusing biomolecules using alternating-laser excitation. *Biophysical Journal*, **88**, 2939-2953.
44. Chernyshev, E.A. and Tolstikova, N.G. (1962) Gas-phase reactions of hydride chlorosilanes with alkylbenzenes and α - and β -chlorostyrenes. *Bulletin of the Academy of Sciences of the USSR Division of Chemical Science*, **11**, 1147-1151.
45. Tsodikov, O.V., Holbrook, J.A., Shkel, I.A. and Record, M.T., Jr. (2001) Analytic binding isotherms describing competitive interactions of a protein ligand with specific and nonspecific sites on the same DNA oligomer. *Biophysical Journal*, **81**, 1960-1969.
46. Royer, C.A. and Scarlata, S.F. (2008) Fluorescence approaches to quantifying biomolecular interactions. *Methods in enzymology*, **450**, 79-106.
47. Andrews, A.J. and Luger, K. (2011) A coupled equilibrium approach to study nucleosome thermodynamics. *Methods in enzymology*, **488**, 265-285.
48. Fan, J.Y., Zhou, J. and Tremethick, D.J. (2007) Quantitative analysis of HP1 α binding to nucleosomal arrays. *Methods*, **41**, 286-290.